Structure and properties of CoMnSb in the context of half-metallic ferromagnetism

Vadim Ksenofontov,[1] Gennadiy Melnyk,[1] Marek Wojcik,[2] Sabine Wurmehl,[1] Kristian Kroth,[1] Sergey Reiman,[1] Peter Blaha,[3] and Claudia Felser[1]

[1]*Institut für Anorganische Chemie und Analytische Chemie, Johannes Gutenberg-Universität, Staudinger Weg 9, D-55099 Mainz, Germany*

[2]*Institute of Physics, Polish Academy of Sciences, Aleja Lotnikow 32/46, 02-668 Warszawa, Poland*

[3]*Institut für Materialchemie, TU Wien, A-1060 Vienna, Austria*

(Received 10 August 2006; published 25 October 2006)

Although its X-ray powder diffraction patterns show a superstructure, the compound CoMnSb, like the well-known half-Heusler alloy NiMnSb, is often referred to the category of half-metallic ferromagnets with $C1_b$ structure. Our study assigns CoMnSb to space group $Fm\bar{3}m$. The crystal structure of CoMnSb can be represented as an alternation of Co_2MnSb and MnSb structural units, and, in contrast to NiMnSb, displays three Mn and two Sb positions in the elementary cell. The presence of nonequivalent antimony and manganese positions was verified using NMR and Mössbauer spectroscopic measurements. Band-structure calculations based on a proposed structure confirm the experimentally found magnetic moment value of approximately 4 μ_B/f.u. and demonstrate that CoMnSb is not a half-metallic ferromagnet.

DOI: 10.1103/PhysRevB.74.134426 PACS number(s): 75.50.Cc, 72.25.Ba, 71.20.−b, 82.80.Ej

I. INTRODUCTION

Applications involving the spin polarization of carriers now represent a new research field known as magnetoelectronics or spintronics.[1] The predicted advantages of spintronic technology are the nonvolatile storage of data, the high storage density, and the low energy consumption. The fundamentals of spin-polarized transport, the classification of half-metallic materials along with examples, and the projected applications of spin-based devices are discussed in numerous publications.[2,3] The family of half-Heusler compounds provides a variety of half-metallic ferromagnetic materials, which are promising as sources of spin-polarized electrons. Half-Heusler phases *XYZ* (*X* and *Y* are different transition metals, *Z* denotes an *sp* element) can be formally constructed from the Heusler phases X_2YZ by removing one of the two *X* atoms and leaving structural voids. The increase of the distance between *X* neighbors leads to a weaker overlap between 3*d* wave functions and to the presence of gaps in the density of states. This feature gives rise to a large variety of electronic and magnetic properties that range from nonmagnetic semiconductors (CoTiSb) to ferromagnetic half metals (NiMnSb) with complete electron spin polarization at the Fermi level.

De Groot *et al.* have shown that the half-Heusler compound NiMnSb has a gap at the Fermi energy in the minority band.[4] Like NiMnSb, the half-Heusler ferromagnetic compound CoMnSb is often classified in the category of half-metallic ferromagnets.[5] This is because of the apparent resemblance between the structures of these compounds. However, some inconsistencies exist in previous studies regarding the magnetic and structural properties of CoMnSb. Assuming that it was isostructural to NiMnSb, Galanakis estimated the value of the magnetic moment of CoMnSb to be 3 μ_B per f.u., which is in disagreement with the experimentally found magnetization value of ~4 μ_B.[6,7] Band structure calculations for CoMnSb, based on a NiMnSb-like structure and using the augmented plane wave (APW) and Korringa-Kohn-Rostoker (KKR) method, indicate a half-metallic state phase with a total magnetic moment of 3 μ_B.[8,9] In attempting to explain the disagreement with the experimentally measured magnetization value, Toboła and Pierre[6] discussed the presence of a complicated superstructure revealed in an early crystallographic study.[10] In the study presented here, it is concluded that CoMnSb crystallizes in a manner that is different from the way that $C1_b$-type compounds that belong in the $Fd\bar{3}m$ space group crystallize. The doubling of the unit cell parameters is explained by the displacement of Co and Sb atoms from their positions in the $C1_b$ structure. The results of KKR computations, based on a structure that is doubled along the three directions of the fcc unit cell (space group $Fd\bar{3}m$), indicate a half-metallic character for the density of states (DOS) because of a very narrow gap that appears for the spin-down electrons.[6] An integer value of 4 μ_B for the magnetic moment follows from these computations. However, our analysis of the CoMnSb structure shows that the choice of the space group $Fd\bar{3}m$ as proposed in an earlier work[10] is controversial. The value of the coordinate $x=0.2563$, which was chosen in the cited paper, leads to a fourfold overlapping of Sb atoms in the 32*e* fully occupied position and Co atoms in the 8*a* positions. Because of the controversial choice that was made for the space group, we decided to revise the structure and to extend the experimental data to determine if CoMnSb belongs to the class of half-metallic ferromagnets.

II. SAMPLE PREPARATION AND CHARACTERIZATION

A. Synthesis

The three compounds CoMnSb, NiMnSb, and CoTiSb have been synthesized and characterized according to procedures described elsewhere.[11,12] Samples of these compounds, each having a total weight of approximately 1 g, were obtained by arc-melting the proper amounts of the constituents in purified argon. Electrolytically manufactured cobalt

(99.9%), manganese (99.9%), nickel (99.9%), titanium (99.9%), and antimony (99.999% purity) were all supplied by Chempur. To allow for an eventual antimony deficit due to possible evaporation, we started with CoMnSb and increased to $CoMnSb_{1.05}$ compositions in 1% Sb concentration steps. To homogenize the material, polycrystalline samples were annealed for one week at 400 °C in vacuum. For the X-ray powder analysis, we chose a single-phase composition of CoMnSb from the entire series. Because of its sensitivity to impurities that contain antimony, ^{121}Sb Mössbauer spectroscopy was used to characterize the samples.

B. X-ray powder diffraction measurements

Using a Bruker D5000 diffractometer, structural information was obtained by powder diffraction in the transmission mode. For the first step, the positions of the diffraction maxima and the integrated intensities of individual or partly overlapping reflections were determined by using the line-profile approximation method. The data that were obtained were used for indexing, for the subsequent refinement of the unit-cell parameters by the least-squares method, and for the construction of three-dimensional Patterson maps to determine the trial model of the structure. This model was refined by using the full-profile Rietveld method with the simultaneous construction of conventional and difference Fourier maps of the electron density.[13,14] As the final step, the atomic coordinates and the thermal parameters for the atoms were refined. Structure reliability was confirmed by the final values for the corresponding reliability factors $R_{\text{intensity}}=0.0678$ and $R_{\text{profile}}=0.1372$.

C. Magnetic characterization

The magnetic characterization of the samples was performed using a Quantum Design MPMS-XL SQUID magnetometer equipped with a high-temperature furnace. The Curie temperature was determined by heating the CoMnSb sample from 300 K to 775 K in an external field of 1000 Oe. The experimental data were corrected for diamagnetism by using Pascal's constants. The magnetic properties of CoMnSb have been previously reported by Buschow.[11] The saturation magnetization was determined to be 3.93 μ_B/f.u. at 4.2 K. The Curie temperature was found to be 490 K. In this study, we found a saturation magnetization of 3.8(1) μ_B/f.u. at 5 K and a Curie temperature of 481 K. This compound belongs to the class of soft magnetic materials with almost zero remanent magnetization.

D. Mössbauer spectroscopy

^{121}Sb Mössbauer measurements were performed with a constant acceleration Mössbauer spectrometer in a standard transmission geometry using a $^{121m}Sn(CaSnO_3)$ source with a nominal activity of 3 *m*Ci. To increase the recoil-free fraction, both the source and the absorber were immersed in liquid helium. The spectra were analyzed using the transmission integral in the EFFI program.[15] As a constraint, the recoil-free fraction of the source was kept to 0.7.

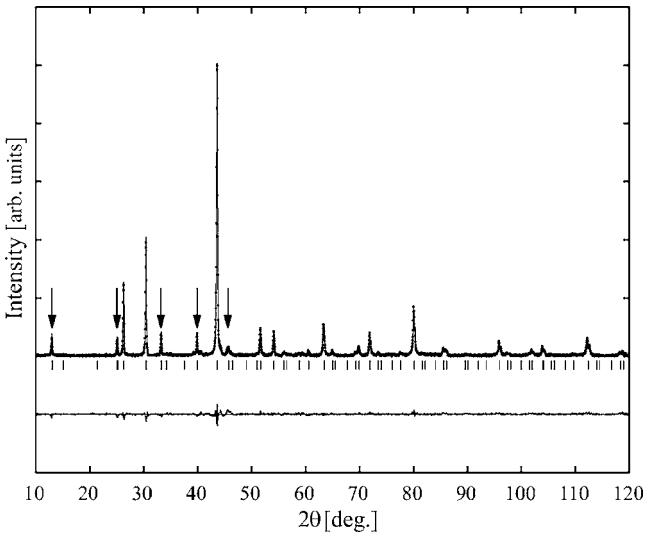

FIG. 1. Powder diffraction patterns (indicated by vertical marks) and Rietveld refinement for CoMnSb. The difference plot is shown at the bottom of the figure. Several intensive superstructure patterns are indicated by arrows.

E. NMR measurements

The NMR experiments were carried out on samples of powdered NiMnSb and CoMnSb at 4.2 K by using a broadband phase-sensitive spin-echo spectrometer.[16] In a zero external magnetic field and a constant rf excitation field, the NMR spectra were recorded for the frequency range 30–450 MHz by measuring the spin-echo intensity in steps of 1 MHz. For field amplitudes that varied more than an order of magnitude, the intrinsic NMR enhancement factors for signals originating from the domain walls of ferromagnetic samples were calculated from the rf field dependencies of the spin-echo intensities.[17] The intensity of a final NMR spectrum, after correction for the enhancement factor and for the usual ω^2 dependence of the spectrum intensity, is proportional to the number of nuclei with a given NMR frequency.

III. RESULTS AND DISCUSSION

According to the analysis of the X-ray powder diffraction measurements presented in Fig. 1, the structure of CoMnSb belongs to the space group $Fm\bar{3}m$, $a=11.7345(3)$ Å. Corresponding crystallographic data, atomic coordinates and interatomic distances within the first nearest-neighbor coordination sphere for CoMnSb are given in Tables I and II. CoMnSb crystallizes into a superstructure with a supercell incorporating eight elementary $C1_b$ cells that can be represented as alternating Co_2MnSb and MnSb structural units (a NaCl-like atom arrangement) in a full Heusler structure (Fig. 2). In NiMnSb, every layer is shifted relative to the previous one by half a period in both directions in the layer plane, whereas in CoMnSb, every two layers are shifted in a similar way. This structural organization leads to the doubling of the period in CoMnSb. In contrast to NiMnSb, the crystal lattice of CoMnSb contains two antimony positions Sb1 and Sb2 at relative populations of 1:3, and three manganese positions

TABLE I. Atomic coordinates and isotropic displacement parameters for CoMnSb.

Atom	Wyckoff position	*X*	*Y*	*Z*	B_{eq}, B_{iso} (Å^2)
Mn1	4*a*	0	0	0	0.70
Mn2	4*b*	1/2	1/2	1/2	1.10
Mn3	24*d*	0	1/4	1/4	0.91
Sb1	8*c*	1/4	1/4	1/4	0.98
Sb2	24*e*	0.7394(2)	0	0	0.71
Co	32*f*	0.1221(3)	*X*	*X*	0.53

Mn1, Mn2, and Mn3 with relative populations of 1:1:6, whereas only one position is observed for Co atoms (Fig. 3).

To verify the structure proposed for CoMnSb, we performed ^{121}Sb Mössbauer spectroscopic and NMR measurements. During the course of the Mössbauer studies, CoTiSb and NiMnSb were also measured for comparison. Mössbauer spectra of CoTiSb (**1**), NiMnSb (**2**), and CoMnSb (**3**) recorded at $T=4.2$ K are shown in Fig. 4. The measurements for (**1**) display a single line spectrum with an isomer shift of $\delta(1)=-5.77(1)$ mm s^{-1} [the isomer shift (IS) values are hereby quoted relative to $Ca^{121m}SnO_3$ at 4.2 K]. This spectrum reflects the paramagnetic state of CoTiSb and does not contain extrinsic phases. The Mössbauer spectrum of (**2**) corresponds to one antimony site with $\delta(\mathbf{2})=-7.52(2)$ mm s^{-1} and a hyperfine magnetic field $H_{hf}(\mathbf{2})=300(2)$ kOe. The Mössbauer spectrum of (**3**) displays a smeared magnetic hyperfine structure that cannot be fit with the only antimony site. In accordance with a proposed structure for CoMnSb, the spectrum was decomposed into two magnetic subspectra **A** and **B** with partial intensities of 25% and 75%. Site **A**, with an isomer shift of $\delta(\mathbf{3A})=-10.4(6)$ mm s^{-1}, an $H_{hf}(\mathbf{3A})=290(3)$ kOe, and a zero value for the quadrupole coupling, corresponds to the regular coordinated position of antimony. Site **B**, with $\delta(\mathbf{3B})=-10.4(1)$ mm s^{-1} and $H_{hf}(\mathbf{3B})=190(5)$ kOe, exhibits a quadrupole splitting $\Delta E_Q(\mathbf{3B})=12.7(9)$ mm s^{-1}, indicating that the local surroundings are distorted. It may be concluded that the model that is obtained by fitting two Sb sites is capable of describing the Mössbauer spectrum of CoMnSb, and supports the existence of two crystallographic sites of antimony following from the structural analysis. Taking into account the partial intensities of the subspectra, we attribute sites **A** and **B** to the Sb1 and Sb2 positions, respectively.

Figure 5 shows the NMR spectra for NiMnSb and CoMnSb. The spectrum for bulk NiMnSb (Fig. 5(a)) can be interpreted in conformity with earlier published studies.[18,19] The dominant NMR line in the spectrum at 300 MHz stems from the ^{55}Mn resonance. Because of the cubic structure of NiMnSb, this line is narrow and is not split. The resonance lines at 165 MHz and 305 MHz may be assigned to ^{123}Sb and ^{121}Sb with a nuclear hyperfine magnetic field of 299 kOe. This value is in fair agreement with a hyperfine magnetic field of 300(2) kOe measured in the Mössbauer experiments. The frequency ratio between the lines at 165 MHz and 305 MHz corresponds exactly to the ratio between the gyromagnetic constants for ^{123}Sb and ^{121}Sb. The ^{61}Ni NMR signal is expected at approximately 23 MHz and was therefore not observed in our experiment. The complicated structure of the CoMnSb NMR spectrum consists of a superposition of broad and relatively narrow resonances and can be separated into three groups of lines that correspond to the three elements comprising CoMnSb. To a first approximation, the intensity ratio for the group should be 1:1:1. The deconvolution of the complete spectrum of CoMnSb (Fig. 5(b)) was performed by using Gaussian peaks. The parameters for the resonance lines are given in Table III. The intense line at 113 MHz is due to the ^{59}Co resonance, whereas the quintet between 212 MHz and 282 MHz is a clear fingerprint of ^{55}Mn ($I=5/2$) experiencing a quadrupole interaction. If second-order quadrupole effects are assumed, then the quintet resonance spectrum of ^{55}Mn is not equidistant.

TABLE II. Interatomic distances (Å) within the first nearest-neighbor coordination sphere for CoMnSb.

Mn1	8Co	2.481(4)	Sb1	4Co	2.601(4)
	6Sb2	3.058(3)		6Mn3	2.9336(3)
Mn2	6Sb2	2.809(3)	Sb2	4Co	2.597(4)
				1Mn2	2.809(3)
				4Mn3	2.9362(3)
				1Mn1	3.058(3)
Mn3	4Co	2.561(4)	Co	1Mn1	2.481(4)
	6Sb2	2.9336(3)		3Mn3	2.561(4)
				3Sb2	2.597(4)
				1Sb1	2.601(4)

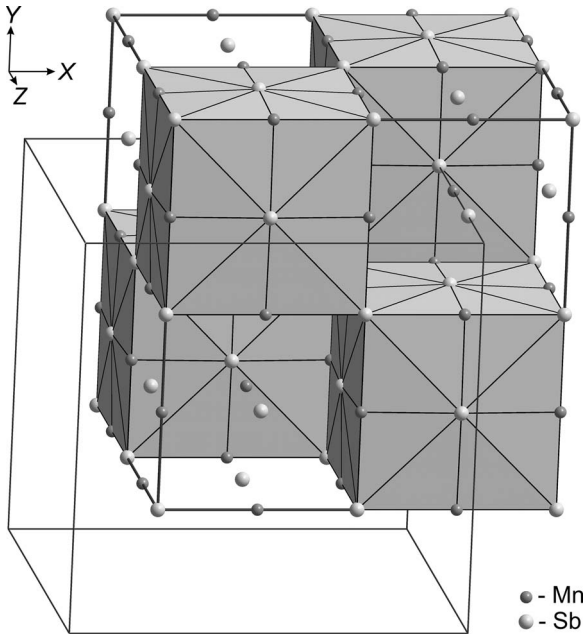

FIG. 2. The CoMnSb structure can be presented as an alternation of Co_2MnSb (shaded volumes) and MnSb structural units. The boundaries of the elementary cell at (1/4,1/4,1/4) are shown shifted relative to the origin.

The average distance between the lines of a quadrupole quintet at 18.0 MHz permits an estimate for the absolute value of the quadrupole splitting $\nu_Q = 3\ eV_{ZZ}Q/2I(2I-1)$ and for the main component V_{ZZ} of the local electric field gradient (EFG) at the manganese atoms. We assume that this NMR signal corresponds to the Mn3 site, because due to symmetry, the Mn1 and Mn2 sites do not have any quadrupole splitting. If the ^{55}Mn quadrupole moment $Q = 0.6 \times 10^{-28}$ m^2, then V_{ZZ}(Mn1) is found to be 1.4×10^{22} V/m^2. The value of the hyperfine magnetic field on Mn3 atoms that show NMR at an

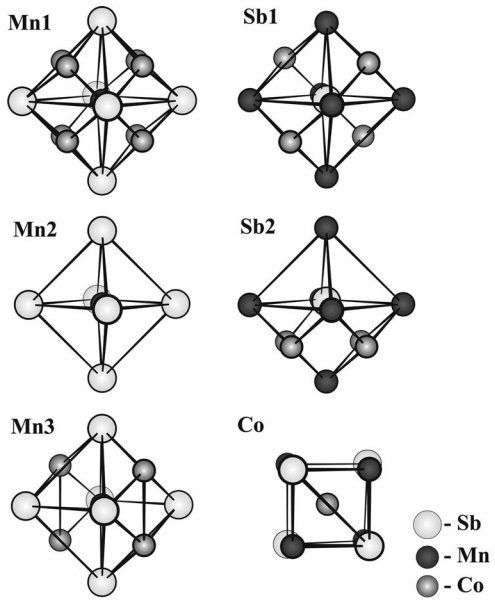

FIG. 3. First coordination polyhedra for the constituent atoms in CoMnSb.

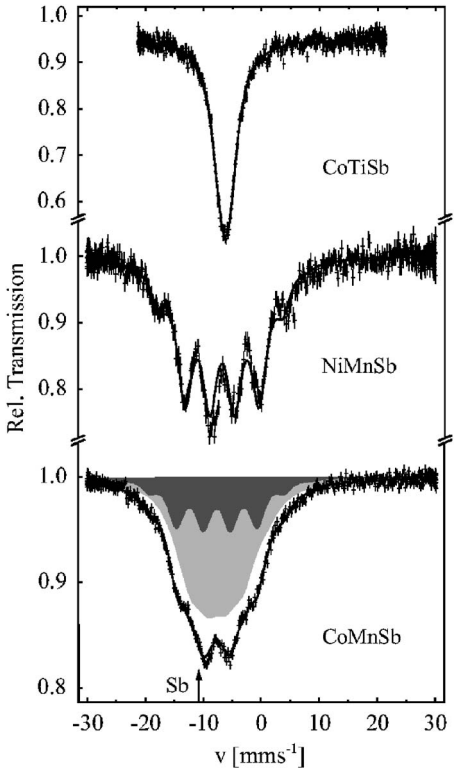

FIG. 4. ^{121}Sb Mössbauer spectra of CoTiSb, NIMnSb, and CoMnSb recorded with the source $^{121m}Sn(CaSnO_3)$ and absorbers at 4.2 K. The CoMnSb spectrum reveals two antimony sites. As a reference, the line position of antimony metal is indicated by an arrow [δ(Sb) = −10.84(2) mm s^{-1}, T = 4.2 K].

average resonance frequency of 247 MHz is 234 kOe (γ = 1.0553 kHz Oe^{-1}). The third group, which consists of the broad lines located at 297 MHz, 196 MHz, 154 MHz, and 102 MHz, may be assigned to the NMR on the ^{121}Sb and ^{123}Sb nuclei that are experiencing hyperfine magnetic fields of 291 kOe and 192 kOe, respectively (Table III). The main support for this assignment comes from Mössbauer spectroscopic measurements that indicate two ^{121}Sb positions with H_{hf} = 290(3) kOe and H_{hf} = 190(5) kOe. The broad line in the high-frequency part of the spectrum centred at H_{hf} = 365 MHz may be attributed to NMR signals from Mn1 and Mn2atoms. In summary, the main results gained from NMR experiments with CoMnSb are the following: (i) Sb atoms experience a magnetic interaction and occupy two crystallographic sites; (ii) magnetic cobalt atoms occupy a unique position that shows no apparent quadrupole splitting; and (iii) Mn atoms provide two groups of signals. The more intense ^{59}Mn signal corresponds to the Mn3 site and shows a pronounced quadrupole splitting that indicates a noncubic crystal field symmetry. The NMR signals for the Mn1 and Mn2 sites show a broad line centered at 365 MHz.

To interpret the hyperfine parameters on the atoms that comprise CoMnSb, we performed calculations using the WIEN2K package[20,21] based on the full-potential, linear-augmented-plane-wave method. According to these calculations, EFG at Mn3 has a main component V_{ZZ} = 0.810^{22} V/m^2 and an asymmetry parameter η = 0.86. The value for the EFG is of the same order of magnitude as the

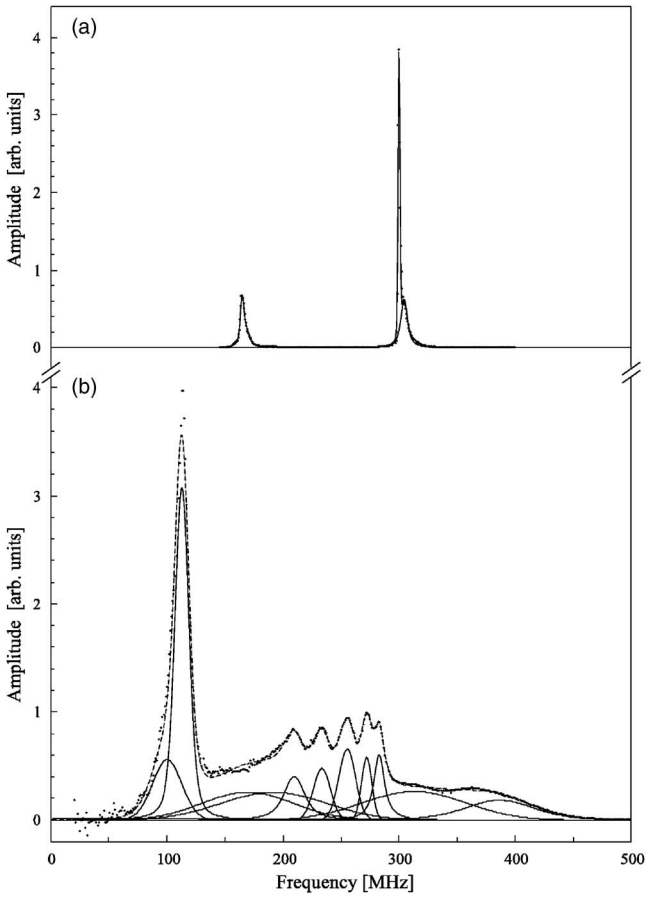

FIG. 5. NMR spectra of NiMnSb (a) and CoMnSb (b). A detailed assignment of the resonance lines for CoMnSb is given in Table III.

experimentally observed $V_{zz}=1.4\times10^{22}$ V/m^2. Calculations show that Co atoms should have a much smaller EFG of $V_{ZZ}=-1.44\times10^{21}$ V/m^2 (with $\eta=0$). In fair agreement with experiment, the ^{59}Co NMR line does not display a noticeable multiplet structure. The first coordination sphere of Sb2 positions consists of four Co atoms and six manganese positions filled by Mn1, Mn2, and Mn3 (Fig. 3). The sign of the quadrupole splitting for the Sb2 position in CoMnSb from the Mössbauer experiment coincides with the sign obtained from calculations. Since the sign of the quadrupole moment for ^{121}Sb is negative,[22] the experimentally found positive quadrupole splitting for Sb2 indicates a negative sign for the principal component of the electric field gradient, which is in agreement with the calculated value of $V_{ZZ}=-0.8\times10^{22}$ V/m^2. However, this value is in apparent disagreement with a value of $V_{ZZ}=-6\times10^{22}$ V/m^2 from the Mössbauer measurements and cannot be verified by NMR because of the broad overlapping resonance lines and the complicated structure of the CoMnSb NMR spectrum. The disagreement between the experimental and calculated hyperfine magnetic fields found at the nuclei may be considered to be a complicated problem. WIEN2K calculations for the hyperfine magnetic field at antimony sites in NiMnSb yield a value of 450 kOe, which is quite different from the experimentally measured value of $H_{hf}\cong300$ kOe. In contrast to the measured values of H_{hf}(Sb1)=290(3) kOe and H_{hf}(Sb2)=190(5) kOe, calculations for CoMnSb give values for the hyperfine fields of H_{hf}(Sb1)=231 kOe and H_{hf}(Sb2)=391 kOe. The calculated values for the hyperfine fields on the Mn atoms in CoMnSb are −134 kOe (Mn1), −53 kOe (Mn2), −59 kOe (Mn3), and are not confirmed experimentally by ^{55}Mn NMR measurements. However, the calculations for the hyperfine field on Co atoms in CoMnSb gave a value of −109 kOe, which is in good agreement with NMR measurements (Table III). A possible reason for the difficulties in evaluating the hyperfine magnetic fields in CoMnSb may be that H_{hf} is very sensitive to the parameters used in the calculation model, and that even small differences in the effects of fields of opposite sign, created by the action of magnetically polarized *s*-electron pairs of internal shells at nuclei, can account for fields of hundreds of kilo-Oersteds.[24] It can be concluded that calculating the magnetic fields at nuclei is a complicated task, and that the discrepancy between the theoretical and experimental values of hyperfine fields may be classified as a general problem for which there is not as yet any satisfactory solution.

TABLE III. NMR frequencies, hyperfine fields, and corresponding site assignments in CoMnSb.

Frequency (MHz)	Nucleus (site)	Hyperfine field (kOe)
365	^{55}Mn (Mn2, Mn3)	346
297	^{121}Sb (Sb1)	291
282, 271, 255, 234, 212	^{55}Mn (Mn1)	234
196	^{121}Sb (Sb2)	192
154	^{123}Sb (Sb1)	291
113	^{59}Co	112
102	^{123}Sb (Sb2)	192

Based on the NiMnSb structural model for half-metallic compounds, the expected total magnetic moment for CoMnSb is 3 μ_B.[23,25] Based on the structure proposed in this study, electronic structure calculations for CoMnSb indicate metallic behavior and a total moment of nearly 4 μ_B. The local Co magnetic moment is approximately 0.55 μ_B; the magnetic moment at the Mn1 site is smaller (2.74 μ_B) than the magnetic moments at the Mn2 and Mn3 sites (3.24 and 3.64 μ_B, respectively). Both Sb sites display a small negative moment (−0.05 μ_B) that originates from the 5*p* electrons while the 5*s* electrons show a small positive polarization that results in the positive hyperfine field.

The calculated spin-dependent DOS for ordered CoMnSb is shown in Fig. 6. It may be seen that the Fermi level is located at the conduction band and that a gap is absent. This result is in agreement with the experimentally observed metallic character of CoMnSb. The slightly lower experimental value of 3.8 μ_B for the magnetic moment can be explained as being caused by disorder, similar to the results obtained from calculations of the total and partial DOS for disordered $(Co_{0.5}\square_{0.5})_2$MnSb with vacancies (□).[9] Our simulations of X-ray powder diffraction experiments indicate that partial Co-Mn antisite disordering has no influence on the existence of superstructure reflexes and their positions.

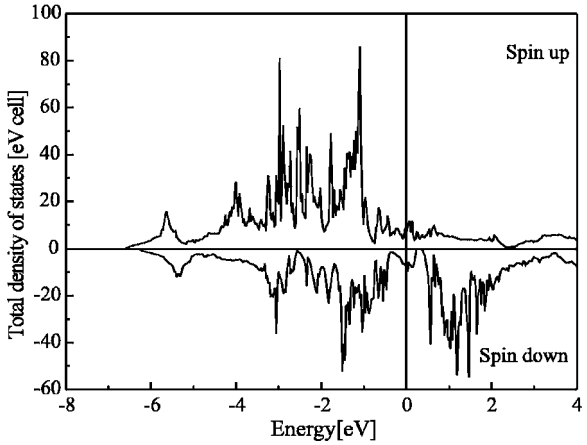

FIG. 6. The spin-dependent DOS of ordered CoMnSb calculated using WIEN2K. The vertical line indicates the Fermi level.

IV. CONCLUSIONS

Because of its hypothetical $C1_b$ structure, half-metallic behavior was commonly postulated for the half-Heusler compound CoMnSb. This compound has 21 valence electrons and, in accordance with the Slater-Pauling rule, it should have a total magnetic moment per unit cell of $M=Z-18=3\ \mu_B$ if it is a half metal.[23] The hypothesis that the structure of CoMnSb, because of its half-Heusler structure, can be described by a $2\times2\times2$ supercell, where half of the Co atoms are put into the "vacancy" positions, was originally discussed in Ref. 9. Our study confirms the period doubling in CoMnSb but indicates a different structure. The crystal structure of CoMnSb is based on the space group $Fm\bar{3}m$ and is formed from alternating Co_2MnSb and MnSb structural units. This crystal structure contains nonequivalent antimony positions that are found in the ^{121}Sb Mössbauer spectroscopic measurements and that are confirmed by NMR. An important argument in favor of the proposed structure for CoMnSb is the nonequivalence of Mn atoms that is found by ^{55}Mn NMR measurements. Band-structure calculations based on the proposed structure do not show a gap in any partial DOS, confirm the metallic character of CoMnSb, and are in agreement with the experimental value of approximately 4 μ_B for the magnetic moment. It is yet to be explained why CoMnSb may have a structure that is different from the expected structure. Studying compositions of $Ni_{1-x}Co_xMnSb$ may be informative in clarifying the mechanisms responsible for the hypothetical structural transformation $F\bar{4}3m$-$Fm\bar{3}m$.

ACKNOWLEDGMENTS

This work is supported by DFG research group No. 559. We gratefully acknowledge financial help from the Materialwissenschaftliches Forschungszentrum der Universität Mainz. The authors thank H. Spiering for assistance in computations using the EFFI program.

[1] G. A. Prinz, Science **282**, 5394 (1998).
[2] J. M. D. Coey, M. Venkatesan, and M. A. Bari, Lect. Notes Phys. **595**, 377 (2002).
[3] I. Žitić, J. Fabian, and S. Das Sarma, Rev. Mod. Phys. **76**, 323 (2004).
[4] R. A. de Groot, F. M. Mueller, P. G. van Engen, and K. H. J. Buschow, Phys. Rev. Lett. **50**, 2024 (1983).
[5] I. Galanakis, J. Phys. Condens. Matter **14**, 6329 (2002).
[6] J. Toboła and J. Pierre, J. Alloys Compd. **296**, 243 (2000).
[7] I. Galanakis, Psi-k Newsletter **51**, 105 (2002).
[8] J. Kübler, Physica (Utrecht) **127**, 257 (1984).
[9] K. Kaczmarska, J. Pierre, J. Toboła, and R. V. Skolozdra, Phys. Rev. B **60**, 373 (1999).
[10] J. P. Senateur, A. Rouault, R. Fruchart, and D. Fruchart, J. Solid State Chem. **5**, 226 (1972).
[11] K. H. J. Buschow, J. Magn. Magn. Mater. **38**, 1 (1983).
[12] M. A. Kouacou, J. Pierre, and R. V. Skolozdra, J. Phys. Condens. Matter **7**, 7373 (1995).
[13] B. A. Hunter and C. J. Howard, ANSTO (1998).
[14] L. G. Akselrud, Y. N. Grin, P. Y. Zavalii, V. K. Pecharsky, and V. N. Fundamenskii, *Collected Abstracts of the 12th European Crystallographic Meeting, Moscow 1989* (1989), Vol. 3, p. 155.
[15] H. Spiering, L. Deak, and L. Bottyan, Hyperfine Interact. **125**, 197 (2000).
[16] S. Nadolski, M. Wojcik, E. Jedryka, and K. Nesteruk, J. Magn. Magn. Mater. **140–144**, 2187 (1995).
[17] M. Bibes, L. Balcells, S. Valencia, J. Fontcuberta, M. Wojcik, E. Jedryka, and S. Nadolski, Phys. Rev. Lett. **87**, 067210 (2001).
[18] T. Hihara, M. Kawakami, M. Kasaya, and H. Enokiya, J. Phys. Soc. Jpn. **26**, 1061 (1969).
[19] J. Schaf, K. Le Dang, P. Veillet, and I. A. Campbell, J. Phys. F: Met. Phys. **13**, 1311 (1983).
[20] P. Blaha, K. Schwarz, G. K. H. Madsen, D. Kvasnicka, and J. Luitz, *WIEN2K, An Augmented Plane* Wave+Local *Orbitals Program for Calculating Crystal Properties* (Tech. Universtät, Wien, Austria, 2001), ISBN 3-9501031-1-2.
[21] K. Schwarz and P. Blaha, Comput. Mater. Sci. **28**, 259 (2003).
[22] J. G. Stevens and V. E. Stevens, Mössbauer Effect Data Index, 130 (1975).
[23] I. Galanakis, P. H. Dederichs, and N. Papanikolaou, Phys. Rev. B **66**, 174429 (2002).
[24] R. E. Watson and A. J. Freeman, Phys. Rev. **123**, 2027 (1961).
[25] I. Galanakis, P. H. Dederichs, and N. Papanikolaou, Phys. Rev. B **66**, 134428 (2002).